Nature of intranight optical variability of BL Lacertae

Haritma Gaur,[1]⋆ Alok C. Gupta,[2,1]⋆ R. Bachev,[3]⋆ A. Strigachev,[3] E. Semkov,[3]
M. Böttcher,[4,5] P. J. Wiita,[6] J. A. de Diego,[7] M. F. Gu,[1] H. Guo,[1] R. Joshi,[8]
B. Mihov,[3] N. Palma,[5] S. Peneva,[3] A. Rajasingam[5] and L. Slavcheva-Mihova[3]

[1]*Key Laboratory for Research in Galaxies and Cosmology, Shanghai Astronomical Observatory, Chinese Academy of Sciences, 80 Nandan Road, Shanghai 200030, China*
[2]*Aryabhatta Research Institute of Observational Sciences (ARIES), Manora Peak, Nainital 263002, India*
[3]*Institute of Astronomy and National Astronomical Observatory, Bulgarian Academy of Sciences, 72 Tsarigradsko Shosse Blvd, 1784 Sofia, Bulgaria*
[4]*Centre for Space Research, North-West University, Potchefstroom 2520, South Africa*
[5]*Astrophysical Institute, Department of Physics and Astronomy, Ohio University, Athens, OH 45701, USA*
[6]*Department of Physics, The College of New Jersey, PO Box 7718, Ewing, NJ 08628-0718, USA*
[7]*Instituto de Astronomía, Universidad Nacional Autónoma de México, 04310 México D.F., México*
[8]*Inter-University Centre of Astronomy and Astrophysics (IUCAA), Pune 411007, India*

ABSTRACT

We present the results of extensive multiband intranight optical monitoring of BL Lacertae during 2010–2012. BL Lacertae was very active in this period and showed intense variability in almost all wavelengths. We extensively observed it for a total for 38 nights; on 26 of them, observations were done quasi-simultaneously in *B, V, R* and *I* bands (totalling 113 light curves), with an average sampling interval of around 8 min. BL Lacertae showed significant variations on hour-like time-scales in a total of 19 nights in different optical bands. We did not find any evidence for periodicities or characteristic variability time-scales in the light curves. The intranight variability amplitude is generally greater at higher frequencies and decreases as the source flux increases. We found spectral variations in BL Lacertae in the sense that the optical spectrum becomes flatter as the flux increases but in several flaring states, deviates from the linear trend suggesting different jet components contributing to the emission at different times.

Key words: galaxies: active – BL Lacertae objects: individual: BL Lacertae – galaxies: jets – galaxies: photometry.

1 INTRODUCTION

BL Lacertae is a well-known source which has been used to define a class of active galactic nuclei (AGNs) that, together with flat-spectrum radio quasars, make up the highly variable objects called blazars. The BL Lacertae class is characterized by the absence or extreme weakness of emission lines (with equivalent width in the rest frame of the host galaxy of <5 Å), intense flux and spectral variability across the complete electromagnetic spectrum on a wide variety of time-scales, and highly variable optical and radio polarization (e.g. Wagner & Witzel 1995). A relativistic plasma jet pointing close to our line of sight can account for the observed properties of these objects. BL Lacertae is an optically bright blazar located at $z = 0.0688 \pm 0.0002$ (Miller & Hawley 1977) hosted by a giant elliptical galaxy with $R = 15.5$ (Scarpa et al. 2000). BL Lacertae is an LBL (low-frequency peaked blazar) as its low-energy spectral component peaks at millimetre to micron wavelengths while the high-energy spectral component peaks in the MeV–GeV range. On

some occasions, BL Lacertae has shown broad H α and H β emission lines in its spectrum, raising the issue of its membership in its eponymous class (Vermeulen et al. 1995).

BL Lacertae was observed by several multiwavelength campaigns carried out by the Whole Earth Blazar Telescope (WEBT/GASP; Böttcher et al. 2003; Raiteri et al. 2009, 2010, 2013, Villata et al. 2009 and references therein). BL Lacertae is well known for its intense optical variability on short and intraday time-scales (e.g. Massaro et al. 1998; Tosti et al. 1999; Clements & Carini 2001; Hagen-Thorn et al. 2004) and strong polarization variability (Marscher et al. 2008; Gaur et al. 2014 and references therein). Extensive light curves for BL Lacertae have been presented by many authors and hence, a number of investigations have been carried out to search for the flux variations, spectral changes and any possible periodicities in the light curves (e.g. Racine 1970; Speziali & Natali 1998; Fan, Qian & Tao 2001; Böttcher et al. 2003; Hu et al. 2006). Nesci et al. (1998) found the source to be variable with the amplitudes of flux variations larger at shorter wavelengths. Papadakis et al. (2003) studied the rise and decay time-scales of the source during the course of a single night and found them to increase with decreasing frequency. They also studied the time-lags between the

⋆ E-mail: haritma@shao.ac.cn (HG); acgupta30@gmail.com (ACG); bachevr@astro.bas.bg (RB)

light curves in different optical bands and found the *B* band to lead the *I* band by ∼0.4 h. Villata et al. (2002) carried out a campaign in 2000–2001 with exceptionally dense temporal sampling, which was able to measure intranight flux variations of this blazar. They found the optical spectrum to be only weakly sensitive to the long-term brightness trend and argued that this achromatic modulation of the flux base level on long time-scales is due to variations of the jet Doppler factor. However, the short-term flux variations and especially the bluer-when-brighter trend indicate the importance of intrinsic processes related to the jet emission mechanism (Raiteri et al. 2013; Agarwal & Gupta 2015).

A key motivation of this study is to look for intraday flux and spectral variations in optical bands during the active state of BL Lacertae in 2010–2012. We also studied interband *BVRI* time delays on intraday time-scales of BL Lacertae. As BL Lacertae is a very well known LBL and the optical bands are located above the first peak of the spectral energy distribution, the fast intraday variability (IDV) properties can yield rather direct implications for the nature of the acceleration and cooling mechanisms of the relativistic electron populations. Over the course of 3 yr, we performed quasi-simultaneous optical multiband photometric monitoring of this source from various telescopes in Bulgaria, Greece, India and the USA on intraday time-scales.

The paper is organized as follows. In Section 2, we briefly describe the observations and data reductions. Section 3 discusses the methods of quantifying variability. We present our results in Section 4. Sections 5 and 6 contain a discussion and our conclusions, respectively.

2 OBSERVATIONS AND DATA REDUCTION

Our observations of BL Lacertae started on 2010 June 10 and ran through till 2012 October 26. The entire observation log is presented in Table 1. The observations were carried out at six telescopes in Bulgaria, Greece, India and the USA. The telescopes in Bulgaria, Greece and India are described in detail in Gaur et al. (2012; table 1) and the standard data reduction methods we used at each telescope are given in section 3 of that paper, so we will not repeat them here. During our observations, typical seeing vary between 1 and 3 arcsec. In our observations of BL Lacertae, comparison stars are observed in the same field as that of blazar and their magnitudes are taken from Villata et al. (1998). Finally, we used star C for calibration as it has both magnitude and colour close to those of BL Lacertae during our observations.

At the MDM Observatory on the south-west ridge of Kitt Peak, Arizona, USA, data were taken for limited periods during the nights of 2010 July 3–8 with the 1.3 m McGraw-Hill Telescope, using the Templeton CCD with *B*, *V*, *R* and *I* filters. CCD parameters are described in Table 2. The standard data reduction was performed using IRAF,[1] including bias subtraction and flat-field division. Instrumental magnitudes of BL Lacertae plus four comparison stars in the field (Villata et al. 1998) were extracted using the IRAF package DAOPHOT[2] with an aperture radius of 6 arcsec and a sky annulus between 7.5 and 10 arcsec.

The host galaxy of BL Lacertae is relatively bright; in order to remove its contribution from the observed magnitudes, we first

---

[1] IRAF is distributed by the National Optical Astronomy Observatories, which are operated by the Association of Universities for Research in Astronomy, Inc, under cooperative agreement with the National Science Foundation.
[2] Dominion Astrophysical Observatory Photometry software.

Table 1. Results of IDV of BL Lacertae.

Date	Telescope	Band	F_{Enh}	$F_c(0.001)$	Amp (per cent)	Variable
10.06.2010	A	*R*	1.018	2.386	–	NV
11.06.2010	A	*R*	0.985	2.008	–	NV
12.06.2010	A	*R*	1.034	2.386	–	NV
14.06.2010	A	*R*	1.054	2.076	–	NV
	C	*R*	0.934	2.033	–	NV
18.06.2010	E	*R*	51.328	1.940	6.63	Var
19.06.2010	E	*R*	1.861	1.940	–	NV
20.06.2010	E	*R*	21.725	1.930	3.48	Var
21.06.2010	E	*R*	1.227	1.972	–	NV
22.06.2010	E	*R*	29.890	1.94	5.28	Var
04.07.2010	F	*B*	2.164	2.281	–	NV
		V	2.155	2.481	–	NV
		R	0.146	2.236	–	NV
		I	0.938	2.281	–	NV
05.07.2010	F	*B*	1.527	2.305	–	NV
		V	0.618	2.281	–	NV
		R	0.109	2.258	–	NV
		I	1.052	2.281	–	NV
06.07.2010	F	*B*	32.4002	1.995	35.85	Var
		V	36.577	1.995	38.64	Var
		R	45.931	2.047	35.64	Var
		I	55.757	1.995	34.82	Var
07.07.2010	F	*B*	2.307	2.481	–	NV
		V	2.284	2.305	–	NV
		R	1.611	2.258	–	NV
		I	1.247	2.258	–	NV
08.07.2010	F	*B*	17.271	2.305	14.49	Var
		V	3.824	2.281	13.76	Var
		R	6.864	2.281	12.40	Var
		I	4.720	2.331	10.96	Var
17.07.2011	E	*B*	35.089	3.239	8.23	Var
		V	90.629	3.239	7.28	Var
		R	50.931	3.239	7.20	Var
01.08.2011	D	*B*	1.860	3.932	–	NV
		V	2.774	3.932	–	NV
		R	2.094	3.932	–	NV
		I	1.862	3.932	–	NV
02.08.2011	D	*B*	1.584	6.195	–	NV
		V	4.858	6.195	–	NV
		R	5.322	7.077	–	NV
		I	2.540	7.077	–	NV
04.08.2011	D	*B*	0.907	2.849	–	NV
		V	0.552	2.983	–	NV
		R	1.507	2.983	–	NV
		I	1.346	2.983	–	NV
06.08.2011	D	*B*	0.368	2.736	–	NV
		V	0.300	2.736	–	NV
		R	0.670	2.790	–	NV
		I	0.859	2.849	–	NV
07.08.2011	D	*B*	0.997	3.239	–	NV
		V	7.058	3.239	10.63	Var
		R	7.773	3.239	8.23	Var
		I	2.046	3.239	–	NV
23.08.2011	D	*B*	0.730	2.448	–	NV
		V	4.960	2.448	12.49	Var
		R	8.400	2.448	9.47	Var
		I	5.092	2.448	9.69	Var
24.08.2011	D	*B*	4.035	2.849	13.55	Var
		V	7.389	2.849	11.36	Var
		R	16.187	2.849	11.12	Var
		I	13.665	2.849	9.98	Var

Table 1 – *continued*

Date	Telescope	Band	F_{Enh}	$F_{\text{c}}(0.001)$	Amp (per cent)	Variable
25.08.2011	D	B	11.247	2.790	30.14	Var
		V	56.7659	2.790	26.30	Var
		R	63.145	2.790	25.55	Var
		I	17.878	2.790	24.10	Var
22.09.2011	D	B	1.354	2.639	–	NV
		V	1.565	2.517	–	NV
		R	1.329	2.517	–	NV
		I	0.930	2.517	–	NV
19.10.2011	D	R	0.574	3.239	–	NV
		I	0.841	4.142	–	NV
06.07.2012	E	V	25.590	2.596	6.18	Var
		R	21.632	2.596	6.14	Var
		I	9.829	2.596	5.30	Var
10.07.2012	E	B	16.174	2.983	6.40	Var
		V	57.750	2.913	6.27	Var
		R	28.700	2.913	6.15	Var
		I	11.878	2.913	5.54	Var
07.08.2012	D	B	2.110	3.753	–	NV
		V	0.558	3.932	–	NV
		R	0.638	3.932	–	NV
		I	0.746	3.932	–	NV
12.08.2012	D	B	4.669	3.598	20.67	Var
		V	18.835	3.598	17.35	Var
		R	36.030	3.598	14.52	Var
		I	24.429	3.753	12.43	Var
15.08.2012	D	B	0.670	3.932	–	NV
		V	0.417	3.932	–	NV
		R	0.908	3.932	–	NV
		I	0.754	3.932	–	NV
16.08.2012	D	B	0.908	3.463	–	NV
		V	1.726	3.463	–	NV
		R	1.622	3.463	–	NV
		I	0.764	3.463	–	NV
18.09.2012	D	B	0.540	3.345	–	NV
		V	1.395	3.345	–	NV
		R	1.034	3.345	–	NV
		I	0.678	3.345	–	NV
08.10.2012	C	R	3.007	1.961	7.89	Var
13.10.2012	C	R	6.686	3.239	11.76	Var
17.10.2012	D	B	6.863	3.932	24.58	Var
		V	27.535	3.932	19.40	Var
		R	42.842	3.932	16.02	Var
		I	33.239	3.932	13.18	Var
22.10.2012	D	B	1.383	2.686	–	NV
		V	1.462	2.555	–	NV
		R	10.608	2.555	13.80	Var
		I	10.043	2.555	12.95	Var
23.10.2012	D	B	0.606	2.596	–	NV
		V	3.585	2.481	9.29	Var
		R	5.166	2.517	10.25	Var
		I	3.329	2.481	9.68	Var
26.10.2012	C	R	4.330	2.596	9.42	Var

A: 1.04 metre Samprnanand Telescope, ARIES, Nainital, India
C: 50/70-cm Schmidt Telescope at National Astronomical Observatory, Rozhen, Bulgaria
D: 60-cm Cassegrain Telescope at Astronomical Observatory, Belogradchik, Bulgaria
E: 1.3-m Skinakas Observatory, Crete, Greece
F: 1.3 m McGraw-Hill Telescope, Arizona, USA
F_{Enh}: enhanced F-test values
$F_{\text{c}}(0.001)$: critical values of F distribution at 0.1 per cent;
Amp: variability amplitude
Var/NV: variable/non-variable

de-reddened the magnitudes using the Galactic extinction coefficient of Romero, Cellone & Combi (1998) and converted them into fluxes. We then subtracted the host-galaxy contribution from the observed fluxes in the *R* band by considering different aperture radii used by different observatories for the extraction of BL Lacertae magnitudes, using Nilsson et al. (2007). We inferred the host-galaxy contribution in *B*, *V* and *I* bands by adopting the elliptical galaxy colours of $V - R = 0.61$, $B - V = 0.96$ and $R - I = 0.70$ from Fukugita, Shimasaku & Ichikawa (1995). Finally, we subtracted the host-galaxy contribution in the *B*, *V* and *I* bands in order to avoid host contamination in the extraction of colour indices (CIs).

3 VARIABILITY DETECTION CRITERION

3.1 Power-enhanced *F*-test

The *F*-test, as described by de Diego (2010), provides a standard criterion for testing for the presence of intranight variability. The *F*-statistic is defined as the ratio of two given sample variances such as s_Q^2 for the blazar instrumental light-curve measurements and s_*^2 for that of the standard star, i.e.

$$F = \frac{s_Q^2}{s_*^2}. \tag{1}$$

Usually, two comparison stars in the blazar field are used to calculate F_1 and F_2, and evidence of variability is claimed if both the *F*-tests simultaneously reject the null hypothesis at a specific significance level (usually 0.01 or 0.001; Gaur et al. 2012 and references therein). In this case, the number of degrees of freedom for each sample, ν_Q and ν_* will be the same, and equal to the number of measurements, *N* minus 1 ($\nu = N - 1$).

Recently, de Diego (2014) called this procedure the 'double positive test' (DPT) and pointed out a problem with this procedure that DPT has very low power and in practice, its significance level cannot be calculated. Also, a large brightness difference or some variability in one of the stars may lead to an underestimation of the source's variability with respect to the dimmer or less-variable star. To avoid this issue, we employed the power-enhanced *F*-test using the approach of de Diego (2014) and de Diego et al. (2015). It consists of increasing the number of degrees of freedom in the denominator of the *F*-distribution by stacking all the light curves of the standard stars and it consists in transforming the comparison star differential light curves to have the same photometric noise as if their magnitudes matched exactly the mean magnitude of the target object. The mean brightness of both the comparison star and the target object are matched to ensure that the photometric errors are equal. Including multiple standard stars reduces the possibility of false detections of intranight variability that can be produced by one single peculiar comparison star light curve. More details are provided in de Diego et al. (2015). In the analysis, we used three standard stars B, C and H in the field of BL Lacertae whose brightnesses are very close to the brightness of BL Lacertae. Thus, for the *i*th observation of the light curve of standard star *j*, for which we have N_j data points, we calculate the square deviation as

$$s_{j,i}^2 = (m_{j,i} - \overline{m}_j)^2. \tag{2}$$

By stacking the results of all observations on the total of *k* comparison stars, we can calculate the combined variance as

$$s_{\text{c}}^2 = \frac{1}{(\sum_{j=1}^{k} N_j) - k} \sum_{j=1}^{k} \sum_{i=1}^{N_j} s_{j,i}^2. \tag{3}$$

Table 2. Details of telescopes and instruments.

Telescope:	1.3 m McGraw-Hill Telescope
Chip size:	4064×4064 pixels
Pixel size:	$15 \times 15\ \mu\text{m}^2$
Scale:	0.315 arcsec pixel^{-1}
Field:	21.3 arcmin $\times$ 21.3 arcmin
Gain:	2.2–$2.4\ e^-$/ADU
Read-out noise:	$5\ e^-$ rms

Then, we compare this combined variance with the blazar light-curve variance to obtain the F-value with $\nu_Q = N - 1$ degrees of freedom in the numerator and $\nu_* = k(N - 1)$ degrees of freedom in the denominator. This value is then compared with the $F_{\nu_Q, \nu_*}^{(\alpha)}$ critical value, where α is the significance level set for the test. The smaller the α value, the more improbable it is that the result is produced by chance. If F is larger than the critical value, the null hypothesis (no variability) is discarded. We have performed the F-test at $\alpha = 0.001$ level.

3.2 Discrete Correlation Function

To estimate the variability time-scales in the observed light curves of BL Lacertae and to determine the cross-correlations between different optical bands, we used the Discrete Correlation Function (DCF; Edelson & Krolik [1988](#); Hovatta et al. [2007](#)).

The first step is to calculate the unbinned correlation (UDCF) using the given time series by

$$\text{UDCF}_{ij} = \frac{(a(i) - \bar{a})(b(j) - \bar{b})}{\sqrt{\sigma_a^2 \sigma_b^2}}. \tag{4}$$

Here, $a(i)$ and $b(j)$ are the individual points in two time series a and b, respectively, $\bar{a}$ and $\bar{b}$ are respectively the means of the time series, and σ_a^2 and σ_b^2 are their variances. The correlation function is binned after calculation of the UDCF. The DCF can be calculated by averaging the UDCF values (M in number) for each time delay $\Delta t_{ij} = (t_{bj} - t_{ai})$ lying in the range $\tau - \frac{\Delta \tau}{2} \le t_{ij} \le \tau + \frac{\Delta \tau}{2}$ via

$$\text{DCF}(\tau) = \frac{1}{n} \sum \text{UDCF}_{ij}(\tau), \tag{5}$$

where τ is the centre of a time bin and n are the number of points in each bin. DCF analysis is frequently used for finding the correlation and possible lags between multifrequency AGN data. When the same data train is used, so $a = b$, there is obviously a peak at zero lag and is called Auto Correlation Function (ACF), indicating that there is no time-lag between the two but any other strong peaks in the ACF give indications of variability time-scales.

4 RESULTS

4.1 Flux variations

We extensively observed the source for a total of 38 nights during 2010–2012. During 26 of those nights, we observed the source quasi-simultaneously in the B, V, R and I bands, providing a total of 113 light curves in B, V, R and I. These light curves are displayed in Figs [1](#) and [2](#). The lengths of the individual observations were usually between 2 and 6 h. It is clear from the figures that BL Lacertae was variable from day to day and also on hourly time-scales. We searched for genuine flux variations on IDV

time-scales and found 50 light curves to be variable in the whole set of filters during a total of 19 nights using the enhanced F-test. The intranight variability amplitudes (in per cent) are given by Heidt & Wagner ([1996](#)):

$$\text{Amp} = 100 \times \sqrt{(A_{\max} - A_{\min})^2 - 2\sigma^2}, \tag{6}$$

where $A_{\max}$ and $A_{\min}$ are the maximum and minimum values in the calibrated light curves of the blazar, and σ is the average measurement error. The enhanced F-test values are presented in Table [1](#).

The duty cycle (in per cent; DC) of BL Lacertae is computed following the definition of Romero, Cellone & Combi ([1999](#)) that later was used by many authors (e.g. Stalin et al. [2004](#); Goyal et al. [2012](#) and references therein),

$$\text{DC} = 100 \frac{\sum_{i=1}^{n} N_i (1/\Delta t_i)}{\sum_{i=1}^{n} (1/\Delta t_i)}, \tag{7}$$

where $\Delta t_i = \Delta t_{i,\text{obs}}(1 + z)^{-1}$ is the duration of the monitoring session of a source on the ith night, corrected for its cosmological redshift, z. Since for a given source the monitoring durations on different nights are not always equal, the computation of the DC is weighted by the actual monitoring duration Δt_i on the ith night. N_i is set equal to 1 if IDV was detected by the F-test (given in Table [1](#)), otherwise $N_i = 0$. We found the DC of BL Lacertae to be around 44 per cent.

4.2 Amplitude of variability

When the variability is substantial, the amplitude of variability usually is greater in higher energy bands (B) and smaller in lower energy bands (R) in most of the observations. It has been found by many investigators that amplitude of variability is greater at higher frequencies for BL Lacertaes (Ghisellini et al. [1997](#); Massaro et al. [1998](#); Bonning et al. [2012](#)); however, the amplitude of variability is not systematically larger at higher frequencies is also found on some occasions (Ghosh et al. [2000](#); Ramírez et al. [2004](#)). In a few cases, we found the amplitude of variability in lower energy bands to be comparable to or greater than the amplitude of variability in higher energy bands. Still, because the errors in the B band are higher in these cases, while they are often lower in the lower frequency band, there are some nights during which the statistical significance of the variations falls below our thresholds in B (also sometimes V), when clear variability is detected in R and I bands. Also, differences in the amplitude of variability in various optical bands change from one observation to another. The highest fractional amplitude of variability was found to be $\sim$38 per cent on 2010 July 6, where the source showed an $\sim$0.3 mag change in less than 3.5 h in the V band.

We searched for possible correlations between the variability amplitude and the duration of the observation, as displayed in Fig. [3](#) (left-hand panel). We found a significant positive correlation ($\rho = 0.3306$ with $p = 0.0190$, where ρ and p are the Spearman Correlation coefficient and its p-value, respectively) between them, i.e. the variability amplitude increases with duration of the observation. We conclude that there is an enhanced likelihood of seeing higher amplitudes of variability in longer duration light curves, which is in agreement with the Gupta & Joshi ([2005](#)) report for a larger sample of blazars.

Next, we examined the possible correlation between the amplitude of variability with the source flux (Fig. [3](#), right-hand panel). It can be seen that amplitude of variability decreases as the source flux increases ($\rho = -0.4990$ with $p = 0.0002$). This might be explained
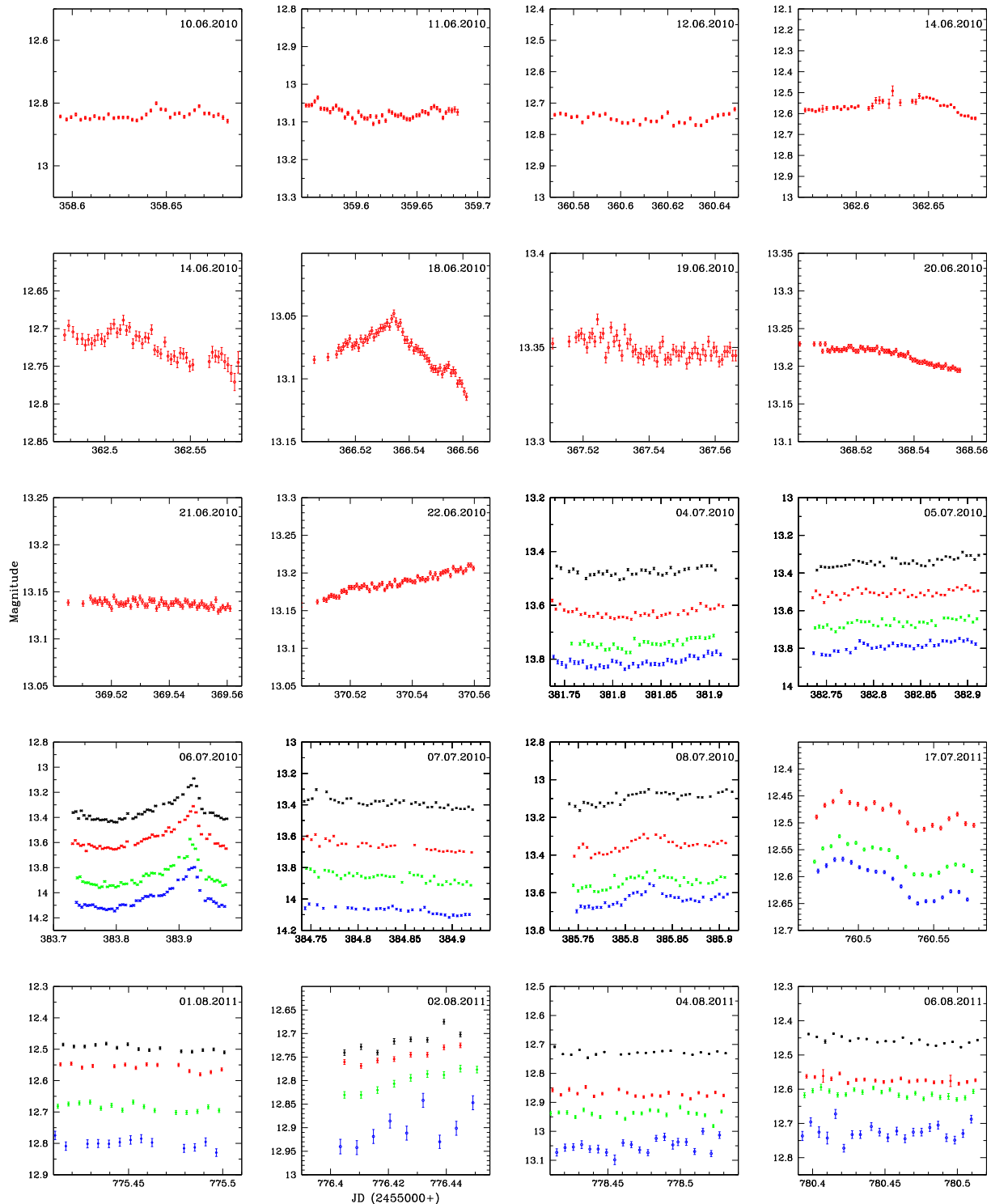
Figure 1. IDV light curves of BL Lacertae during 2010 and early 2011 in the *B* (blue), *V* (green), *R* (red) and *I* (black) bands. The *x*-axis is JD (2455000+), and the *y*-axis is the calibrated magnitudes in each of the panels. The *B*, *V* and *I* bands are shifted by arbitrary offsets with respect to the *R*-band light curve. Observations from observatory A are represented by squares; those from C are represented by triangles; D by filled circles; E by open circles and F by starred symbols.

as, if the source attains a high-flux state, the irregularities in the jet flow decreases particularly if fewer non-axisymmetric bubbles were carried outward in the relativistic magnetized jets (Gupta et al. 2008). For instance, the blazar 3C 279 was observed in 2006 during its outburst/high state but did not show any genuine microvariabil-

ity, while other sources which were in their pre-/post-outburst state showed significant microvariability (Gupta et al. 2008). This anticorrelation between variability amplitude and flux could also be explained by a two-component model where in more active phases or in an outburst state, the slowly varying jet component rises and
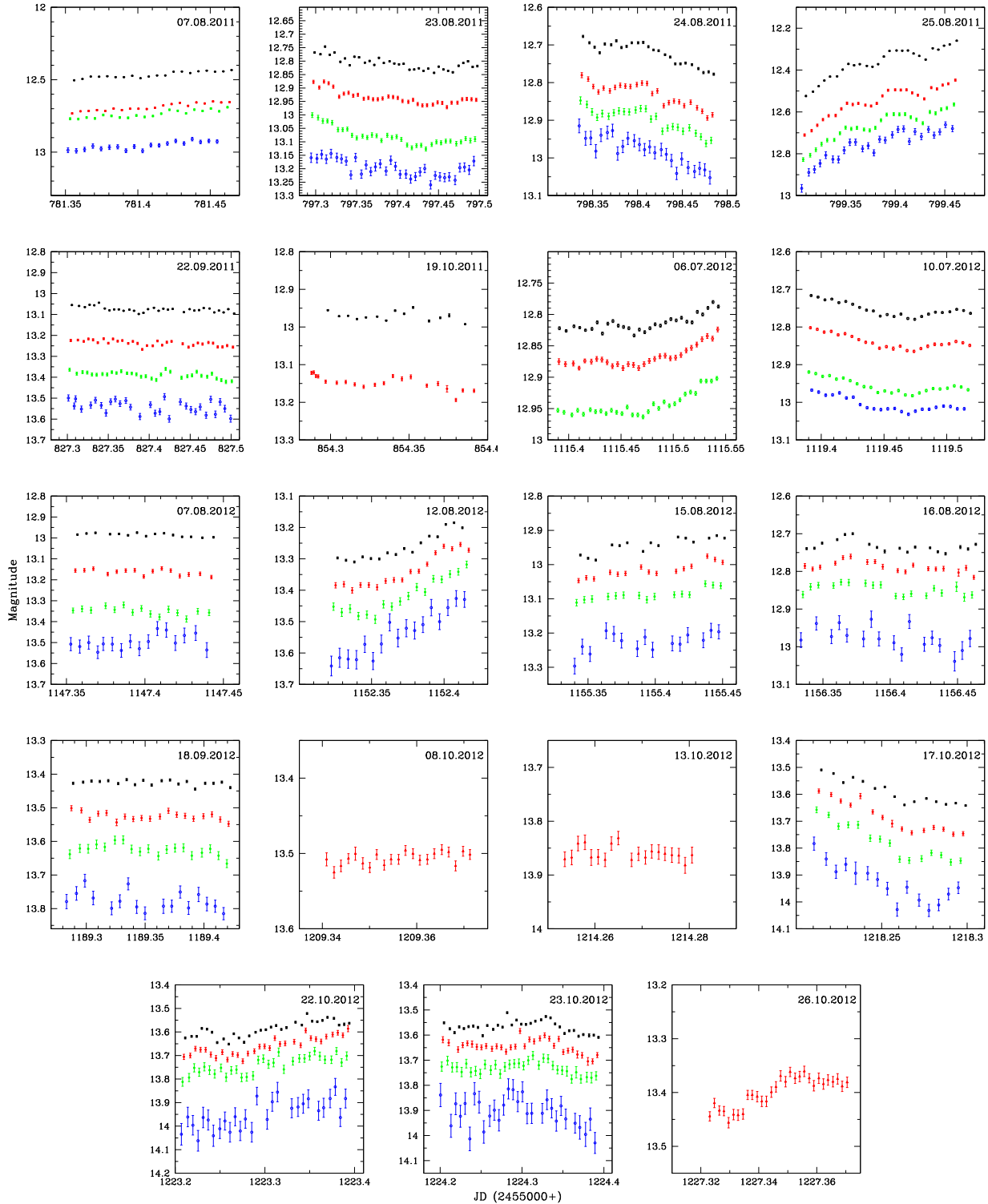
Figure 2. As in Fig. 1 for 2011 August through 2012 October.

dominates on the emission from the more variable regions, i.e. shocks/knots, and therefore reduces the fractional amplitude. However, there is scatter in the plot, some of which could be due to an observational bias, as some observations were longer than others. Due to this, the observed variability amplitude at similar luminosities could be quite different as the amplitude of variability increases with the duration of the observation.

4.3 *R*-band autocorrelations

We searched for the presence of a characteristic time-scale of variability in all of the nights by autocorrelating the *R*-band measurements, for which we had the most data. In most of the nights, the ACF shows a sharp maximum at nearly zero lag, as expected, and it stays positively autocorrelated with itself for time-lags of somewhat less than 1 h followed by dropping to negative values. Hence, we
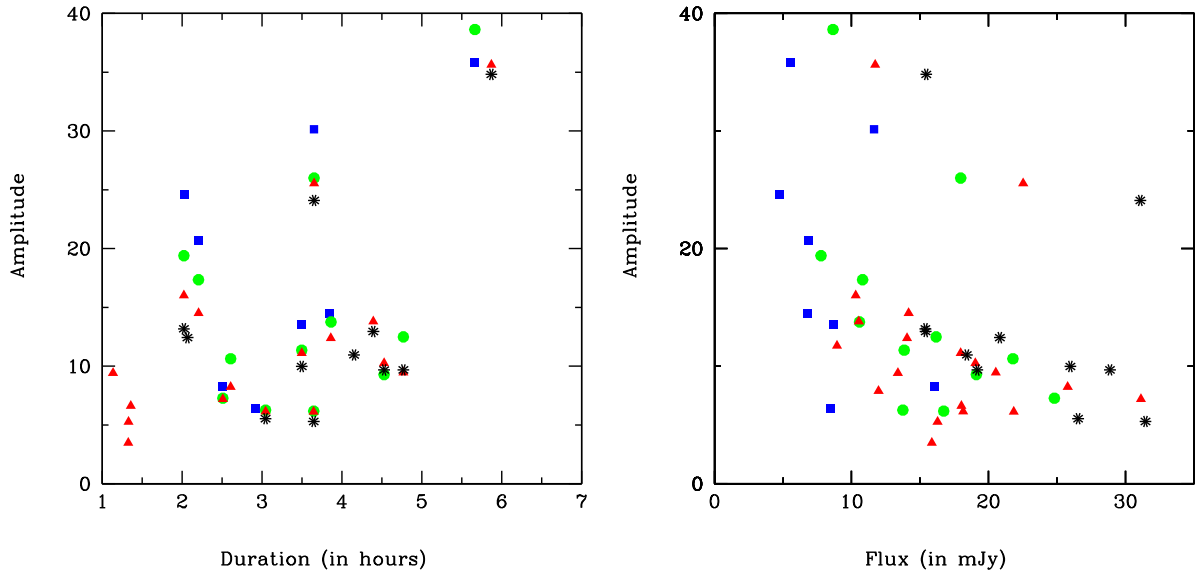
Figure 3. Dependence of amplitude of variability on duration (left-hand panel) and flux (right-hand panel) of the observations. Here, the *B* band is represented by squares (blue), *V* by solid circles (green), *R* by triangles (red) and *I* by starred symbols (black).
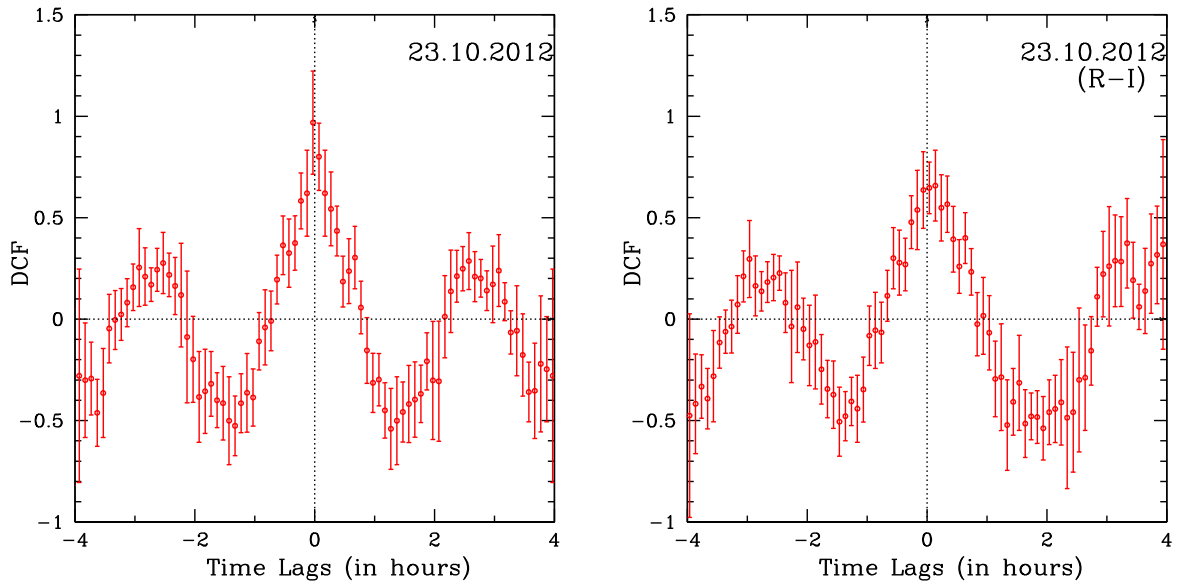
Figure 4. One example of autocorrelation (*R* band) is shown in the left figure and the DCF (*R* versus *I*) is shown in the right figure.

conclude that we did not find any evidence for characteristic variability time-scales from this approach. One example of the *R*-band ACF is shown in the left-hand panel of Fig. 4.

4.4 Interband cross-correlations

We computed the DCFs to determine the cross-correlations and time delays between the *B* and *I*, *V* and *I* and *R* and *I* bands. The time delays are expected between emission in different energy bands, as the flare usually begins at higher frequencies and then propagates to lower frequencies in the inhomogeneous jet model. Injected high-energy electrons emit synchrotron radiation first at higher frequencies and then cool, emitting at progressively lower frequencies, resulting in time-lag between high and low frequencies. The DCFs between the light curves in all bands show close correlations among the various bands in the nights where genuine variability is present.

For the nights in which no genuine variability is present, we normally found much weaker correlations between the bands (<0.4). As the peaks of the DCFs are broad, we fit the DCFs with Gaussian functions to determine the possible time delays; however, lags indicated by the DCFs are all consistent with zero. This is not surprising due to the closeness of the various optical bands we measured in frequency space, so if any lags are present they appear to be less than the resolution of our light curves. An example of the DCF is shown in the right-hand panel of Fig. 4.

4.5 Colour indices (CIs)

We next investigated the existence of spectral variations by studying the behaviour of colour variations with respect to the brightness of BL Lacertae (shown in Fig. 5). The CIs are calculated by combining almost simultaneous (within 8 min) *B*, *V*, *R* and *I* magnitudes to
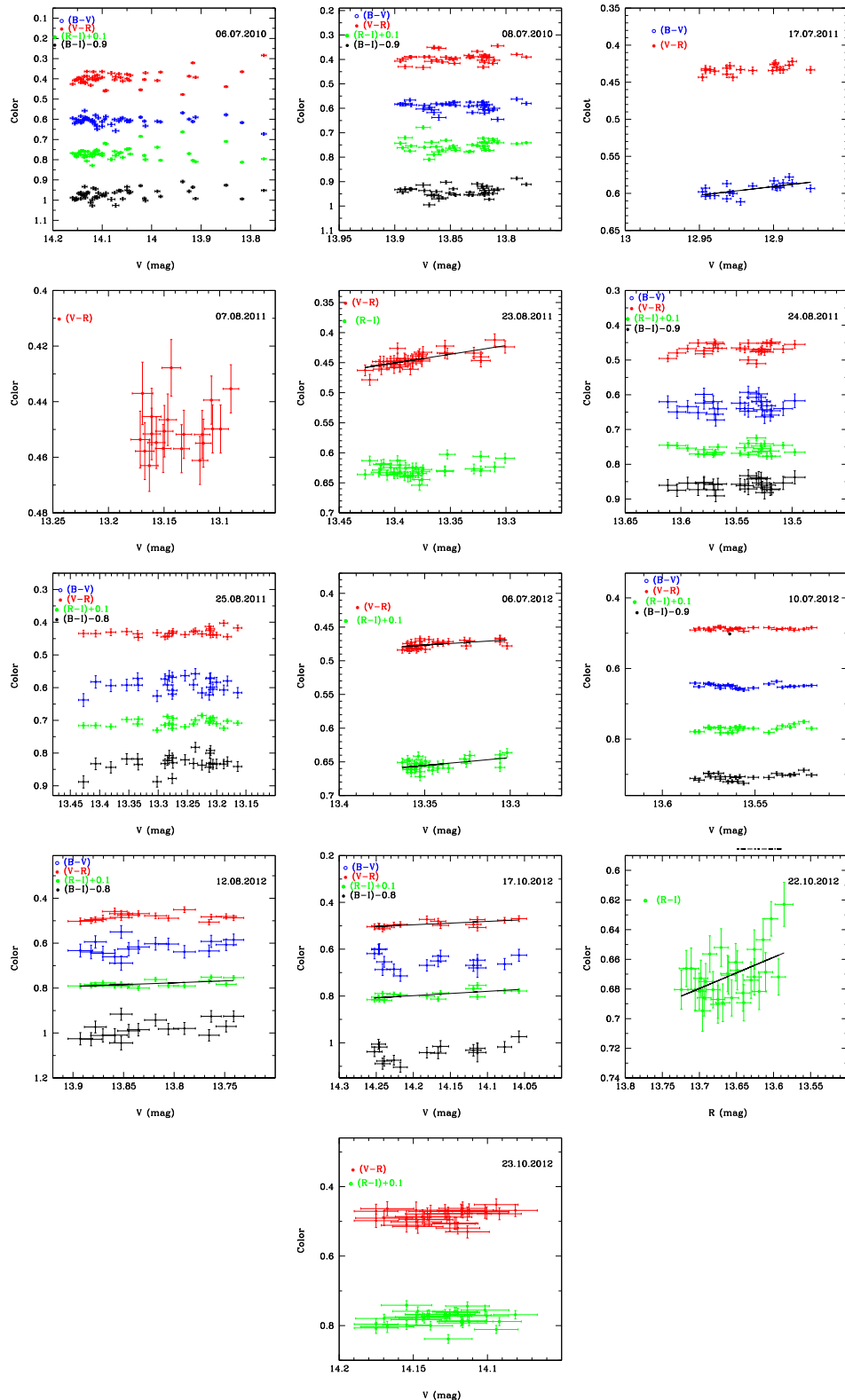
Figure 5. Colour index versus magnitude diagrams for BL Lacertae. The solid line is the best fit on the observations.

yield CIs = $B - V$, $V - R$, $R - I$ and $B - I$. For a particular night, we studied the colour variability only when both light curves were identified as variable. Our data have the advantage of being almost simultaneous in various optical bands. It is important to recall that the underlying host galaxy, effect of the accretion disc component

and the gravitational microlensing can also lead to apparent, but unreal, colour variations (Hawkins 2002). But, since gravitational microlensing is important on weeks to months time-scales and during our observations, BL Lacertae was in flaring state (Raiteri et al. 2013) where the Doppler boosting flux from the relativistic jet

Table 3. Results of linear fits to colour–flux diagrams.

Date of observation	Band	r	p	$c \pm \Delta c$ intercept	$m \pm \Delta m$ slope
06.07.2010	$(B-V)$	-0.138	0.339	1.038 ± 0.446	-0.032 ± 0.032
	$(V-R)$	0.315	0.026	-1.055 ± 0.675	0.110 ± 0.048
	$(R-I)$	0.023	0.873	0.459 ± 0.675	0.008 ± 0.048
	$(B-I)$	0.316	0.026	0.442 ± 0.534	0.087 ± 0.038
08.07.2010	$(B-V)$	-0.106	0.537	1.500 ± 1.455	-0.066 ± 0.105
	$(V-R)$	0.205	0.230	-1.389 ± 1.540	0.136 ± 0.111
	$(R-I)$	0.110	0.545	-0.626 ± 1.836	0.085 ± 0.133
	$(B-I)$	0.220	0.198	-0.516 ± 1.643	0.156 ± 0.119
17.07.2011	$(B-V)^*$	0.629	0.003	-2.424 ± 0.879	0.234 ± 0.068
	$(V-R)$	0.512	0.021	-1.150 ± 0.627	0.123 ± 0.049
07.08.2011	$(V-R)$	0.193	0.415	-0.434 ± 1.058	0.067 ± 0.081
23.08.2011	$(V-R)^*$	0.714	<0.001	-3.423 ± 0.670	0.289 ± 0.050
	$(R-I)$	0.280	0.109	-0.658 ± 0.779	0.096 ± 0.058
24.08.2011	$(B-V)$	0.057	0.788	0.113 ± 1.910	0.038 ± 0.141
	$(V-R)$	0.181	0.388	-0.805 ± 1.446	0.094 ± 0.107
	$(R-I)$	-0.022	0.917	0.787 ± 1.219	-0.009 ± 0.090
	$(B-I)$	0.264	0.202	0.095 ± 1.269	0.123 ± 0.094
25.08.2011	$(B-V)$	0.087	0.673	0.235 ± 0.836	0.027 ± 0.063
	$(V-R)$	0.345	0.118	-0.162 ± 0.366	0.045 ± 0.028
	$(R-I)$	0.251	0.217	0.051 ± 0.439	0.042 ± 0.033
	$(B-I)$	0.325	0.105	0.125 ± 0.894	0.114 ± 0.067
06.07.2012	$(V-R)^*$	0.530	0.003	-1.643 ± 0.641	0.159 ± 0.048
	$(R-I)^*$	0.506	0.004	-2.429 ± 0.994	0.231 ± 0.074
10.07.2012	$(B-V)$	-0.084	0.703	1.019 ± 0.956	-0.027 ± 0.071
	$(V-R)$	0.061	0.781	0.332 ± 0.550	0.011 ± 0.040
	$(R-I)$	0.487	0.019	-2.201 ± 1.125	0.212 ± 0.083
	$(B-I)$	0.395	0.062	-0.850 ± 1.347	0.196 ± 0.099
12.08.2012	$(B-V)$	0.310	0.243	-2.208 ± 2.320	0.205 ± 0.168
	$(V-R)$	0.101	0.709	0.052 ± 1.131	0.031 ± 0.082
	$(R-I)$	0.581	0.011	-1.618 ± 0.861	0.166 ± 0.062
	$(B-I)$	0.517	0.040	-3.774 ± 2.458	0.402 ± 0.178
17.10.2012	$(B-V)$	-0.103	0.716	1.370 ± 1.927	-0.051 ± 0.136
	$(V-R)^*$	0.674	0.006	-1.526 ± 0.614	0.142 ± 0.043
	$(R-I)^*$	0.668	0.006	-1.945 ± 0.816	0.186 ± 0.058
	$(B-I)$	0.542	0.037	-2.102 ± 1.694	0.278 ± 0.120
22.10.2012	$(R-I)^*$	0.482	0.006	-2.203 ± 0.970	0.210 ± 0.071
23.10.2012	$(V-R)$	0.217	0.233	-1.919 ± 1.973	0.170 ± 0.140
	$(R-I)$	0.163	0.373	-1.262 ± 2.147	0.137 ± 0.152

*Significant variations are found in these observations.
r and p: Pearson Correlation Coefficient and its probability values, respectively.

almost invariably swamps out the contribution of the accretion disc component, so we can rule out the contribution of these components. Also, the data we have used in calculating the CIs are host galaxy subtracted, so we conclude that our results indicates variability of the non-thermal continuum radiation.

We studied the variations of CIs with respect to brightness in 13 of these observations. We fit all the colour–magnitude diagrams with a linear model of the form CI = $m \times$ mag + c (where m is the slope in the fit, V magnitude is taken as mag and c is its respective intercept). The Pearson correlation coefficient (r), its p-value (null hypothesis probability; we consider a confirmed colour index correlation with the V magnitude when $p < 0.01$) along with the slopes and intercepts are presented in Table 3. The significant positive correlations between the colour index and magnitude along with a change of slope $>3\sigma$ indicates that the source exhibits a bluer-when-brighter trend.

In five of the nights, which are marked by asterisks in Table 3, we found significant variations in CIs at the 3σ level. In these observations, CIs correlate with the source brightness and the overall correlation is positive, which indicates hardening of the spec-

trum as the source brightens. So, in these observations, BL Lacertae exhibits bluer-when-brighter trend with different regression slopes. No significant negative correlations are found for the source. The bluer-when-brighter tendency in BL Lacertae has been seen by several groups on long-term as well as short-term time-scales (e.g. Papadakis et al. 2003; Villata et al. 2004; Gu et al. 2006; Stalin et al. 2006; Larionov, Villata & Raiteri 2010; Gaur et al. 2012; Wierzcholska et al. 2015). Villata et al. (2004) characterized the intraday flares to be strong bluer-when-brighter chromatic events with a slope of ∼0.4. In five observations, we found a bluer-when-brighter trend with a slope varying between 0.18 and 0.28 (in Table 3).

In the other eight observations, we did not find significant linear correlations between CIs and magnitudes (Table 3). In some of them, significant colour variations are seen but are not well fitted by linear functions. During the observations on 2010 July 6 (Fig. 1, fourth panel), we found a strong flare with magnitude variation of ∼0.3 in all the optical bands and the behaviour of the colour–magnitude diagram varies according to the different flux states. But, on intraday time-scales, it is difficult to judge the variations of the

CIs with respect to different brightness states as the flare is on hours like time-scales. Also, in other observations, i.e. 2010 July 8, 2011 August 24 and 25, we saw small sub-flares superimposed on the long-term trend. In these cases, the CIs vary significantly within the individual observations, sometimes showing different branches in the colour–magnitude diagrams according to the flux states. Spectral steepening during the flux rise can be explained by the presence of two components, one variable with a flatter slope which dominates during the flaring states and another one that is more stable and contributes to the long-term achromatic emission (Villata et al. 2004). So, it could be possible that during these observations, the superposition of many distinct new variable components lead to the overall weakening of the colour–magnitude correlations. Bonning et al. (2012) studied a sample of Flat Spectrum Radio Quasar (FSRQs) and BL Lacertaes and found that FSRQs follow redderwhen-brighter trends while BL Lacertaes show no such trends. They found complicated behaviour of the blazars on colour–magnitude diagrams: hysteresis tracks, and achromatic flares which depart from the trend suggesting different jet components becoming important at different times. Therefore, our colour variability results show that the intranight flares between 2010 and early 2012 are chromatic but do not always follow simple bluer-when-brighter trends.

5 DISCUSSION

We performed photometric monitoring of BL Lacertae during the period 2010–2012 for a total of 38 nights in the B, V, R and I bands in order to study its flux and spectral variability. In 19 of those nights, we found genuine IDV. The light curves often show gradual rises and decays, sometimes with smaller sub-flares superimposed. No evidence for periodicity or other characteristic time-scales was found. We find the DC of the source during this period to be ∼44 per cent. In the earlier studies, it has been found that LBLs display stronger IDV than HBLs (high-frequency peaked blazars) and the DC has been estimated to be ∼70 per cent for LBLs and ∼30–50 per cent for HBLs (Heidt & Wagner 1998; Romero et al. 2002; Gopal-Krishna et al. 2003). Gopal-Krishna et al. (2011) studied a large sample of blazars and found that if variability amplitude (Amp) >3 per cent is considered, the DC is 22 per cent for HBLs and 50 per cent for LBLs. We found DC of ∼44 per cent for BL Lacertae (which is a well-known LBL) is in accordance with the previous studies.

In the literature, there are various models which explains IDV of blazars. Intrinsic ones focus on the evolution of the electron energy density distribution of the relativistic particles leading to a variable synchrotron emission, with shocks accelerating turbulent particles in the plasma jet which then cools by synchrotron emission (e.g. Marscher, Gear & Travis 1992; Marscher 2014; Calafut & Wiita 2015). Extrinsic ones involve geometrical effects like swinging jets where the path of the relativistic moving blobs along the jet deviated slightly from the line of sight, leading to a variable Doppler factor (e.g. Gopal-Krishna & Wiita 1992). The long-term periodic and achromatic BL Lacertae variability may be mostly explained by the geometrical scenarios where viewing angle variation can be due to the rotation of an inhomogeneous helical jet which causes variable Doppler boosting of the corresponding radiation (Larionov et al. 2010, Villata et al. 2002 and references therein). As we are considering the faster intranight flux variations that are associated with the colour variations, they are more likely to be associated with models involving shock propagating in a turbulent plasma jet.

When variability is clearly detected, its amplitude is usually greater at higher frequencies, which is consistent with previous studies (Papadakis et al. 2003; Hu et al. 2006) and can be well

explained by electrons that are accelerated at the shock front and then lose energy as they move away from the front. Higher energy electrons lose energy faster through the production of synchrotron radiation, and are produced in a thin layer behind the shock front. In contrast, the lower frequency emission is spread out over a larger volume behind the shock front (Marscher & Gear 1985). This leads to time-lags of the peak of the light curves towards lower frequencies and amplitude of variability higher at higher frequencies which is clearly visible in the multifrequency blazars light curves. Due to the closeness of the various optical bands, the starting time of a flare should be almost the same and hence on short time-scales, it is difficult to detect the time-lags between the optical bands. Although the amplitude of variability is an inherent property of the source, we had to examine whether it has any dependence on the duration of observation, and found a significant positive correlations between the observed amplitude of variability of the light curves and the duration of the observations. As noted by Gupta & Joshi (2005), on intraday time-scales, the probability of seeing a significant IDV generally increases if the source is continuously observed for long durations. In our observations, duration of monitoring varies between 1.5–5.8 h. Also, we found that the amplitude of variability decreases as the source flux increases which can be explained as the source flux increases, the irregularities in the turbulent jet (Marscher 2014) decrease and the jet flow becomes more uniform leading to a decrease in amplitude of variability.

We searched for the possible correlations between colour versus magnitude and found significant positive correlations between them in five of the observations out of total 13. So, BL Lacertae showed significant bluer-when-brighter trends on these night with different regression slopes (in Table 3). This behaviour is very well known for BL Lacertaes and can be interpreted as resulting from rapid, impulsive injection/acceleration of relativistic electrons, followed by subsequent radiative cooling (e.g. Böttcher & Chiang 2002). However, other observations do not show significant linear correlations and show complicated behaviour on colour–magnitude diagrams, i.e. different slopes according to the different flux states or nearly zero slopes between colour and magnitude (Table 3). Of course it is possible that superposition of different spectral slopes from many variable components (standing shocks in different parts of the jet) could lead to the overall weakening of the colour–magnitude correlations (Bonning et al. 2012).

Hence, the behaviour of the colour–magnitude diagrams provides us with indirect information on the amplitude difference and time-lags between these bands as Dai et al. (2011) performed simulations to confirm that both the amplitude differences and time delays between variations at different wavelengths result in a hardening of the spectrum during the flare rise. They showed that if there is a difference in amplitude in two light curves, it leads to the evolution of the object along a diagonal path in the colour–magnitude diagram. If there is a time-lag along with the amplitude change, counter-clockwise loop patterns on the colour index–magnitude diagram arise (Dai et al. 2011). However, any such lags are probably shorter than the sampling time of our observations, so we are not able to detect them through the DCFs we computed.

6 CONCLUSIONS

Our conclusions are summarized as follows.

(i) During our observations in 2010–2012, BL Lacertae was highly variable in B, V, R and I bands. The variations were well correlated in all four bands and were very smooth, with gradual

rises/decays. In one of the observations, on 2010 October 6, we found a pronounced flare-like event, and the highest variability amplitude is found in the *V* band at 38 per cent.

(ii) In the cases with significant variability, the amplitude of variability is highest in the highest energy band.

(iii) The amplitude of variability correlates positively with the duration of the observation and decreases as the flux of the source increases.

(iv) We searched for time delays between the *B*, *V*, *R* and *I* bands in our observations, but we did not find any significant lags. This implies that the variations are almost simultaneous in all of the bands and any time-lags, if present, are less than our data sampling interval of ∼8 min.

(v) The flux variations are associated with spectral variations on intraday time-scales. In 5 of the 13 observations, the optical spectrum showed the overall bluer-when-brighter trend which could well represent highly variable jet emission.

(vi) The colour versus magnitude diagrams show different behaviours which could represent the contribution of different variable components during the flaring states.

(vii) We conclude that the acceleration and cooling time-scales are very short for these optical variations and hence dense optical observations with even shorter cadence and higher sensitivity are required to better characterize them.

ACKNOWLEDGEMENTS

REFERENCES

Agarwal A., Gupta A. C., 2015, MNRAS, 450, 541
Bonning E. et al., 2012, ApJ, 756, 13
Böttcher M., Chiang J., 2002, ApJ, 581, 127
Böttcher M. et al., 2003, ApJ, 596, 847
Calafut V., Wiita P. J., 2015, JA&A, 36, 255
Clements S. D., Carini M. T., 2001, AJ, 121, 90
Dai Y., Wu J., Zhu Z.-H., Zhou X., Ma J., 2011, AJ, 141, 65
de Diego J. A., 2010, AJ, 139, 1269
de Diego J. A., 2014, AJ, 148, 93
de Diego J. A., Polednikova J., Bongiovanni A., Pérez García A. M., De Leo M. A., Verdugo T., Cepa J., 2015, preprint (arXiv:1505.02113)
Edelson R. A., Krolik J. H., 1988, ApJ, 333, 646
Fan J. H., Qian B. C., Tao J., 2001, A&A, 369, 758
Fukugita M., Shimasaku K., Ichikawa T., 1995, PASP, 107, 945
Gaur H. et al., 2012, MNRAS, 420, 3147

Gaur H., Gupta A. C., Wiita P. J., Uemura M., Itoh R., Sasada M., 2014, ApJ, 781, L4
Ghisellini G. et al., 1997, A&A, 327, 61
Ghosh K. K., Ramsey B. D., Sadun A. C., Soundararajaperumal S., Wang J., 2000, ApJ, 537, 638
Gopal-Krishna, Wiita P. J., 1992, A&A, 259, 109
Gopal-Krishna, Stalin C. S., Sagar R., Wiita P. J., 2003, ApJ, 586, L25
Gopal-Krishna, Goyal A., Joshi S., Karthick C., Sagar R., Wiita P. J., Anupama G. C., Sahu D. K., 2011, MNRAS, 416, 101
Goyal A., Gopal-Krishna, Wiita P. J., Anupama G. C., Sahu D. K., Sagar R., Joshi S., 2012, A&A, 544, A37
Gu M. F., Lee C.-U., Pak S., Yim H. S., Fletcher A. B., 2006, A&A, 450, 39
Gupta A. C., Joshi U. C., 2005, A&A, 440, 855
Gupta A. C. et al., 2008, AJ, 136, 2359
Hagen-Thorn V. A. et al., 2004, Vizier Online Data Catalog, 903, 243
Hawkins M. R. S., 2002, in Green R. F., Khachikian E.Ye., Sanders D.B., eds, ASP Conf. Ser. Vol. 284, IAU Colloq. 184: AGN Surveys. Astron. Soc. Pac., San Francisco, p. 351
Heidt J., Wagner S. J., 1996, A&A, 305, 42
Heidt J., Wagner S. J., 1998, A&A, 329, 853
Hovatta T., Tornikoski M., Lainela M., Lehto H. J., Valtaoja E., Torniainen I., Aller M. F., Aller H. D., 2007, A&A, 469, 899
Hu S. M., Wu J. H., Zhao G., Zhou X., 2006, MNRAS, 373, 209
Larionov V. M., Villata M., Raiteri C. M., 2010, A&A, 510, A93
Marscher A. P., 2014, ApJ, 780, 87
Marscher A. P., Gear W. K., 1985, ApJ, 298, 114
Marscher A. P., Gear W. K., Travis J. P., 1992, Variability of Blazars. Cambridge Univ. Press, Cambridge, p. 85
Marscher A. P. et al., 2008, Nature, 452, 966
Massaro E., Nesci R., Maesano M., Montagni F., D'Alessio F., 1998, MNRAS, 299, 47
Miller J. S., Hawley S. A., 1977, ApJ, 212, L47
Nesci R., Maesano M., Massaro E., Montagni F., Tosti G., Fiorucci M., 1998, A&A, 332, L1
Nilsson K., Pasanen M., Takalo L. O., Lindfors E., Berdyugin A., Ciprini S., Pforr J., 2007, A&A, 475, 199
Papadakis I. E., Boumis P., Samaritakis V., Papamastorakis J., 2003, A&A, 397, 565
Racine R., 1970, ApJ, 159, L99
Raiteri C. M. et al., 2009, A&A, 507, 769
Raiteri C. M. et al., 2010, A&A, 524, A43
Raiteri C. M. et al., 2013, MNRAS, 436, 1530
Ramírez A., de Diego J. A., Dultzin-Hacyan D., González-Pérez J. N., 2004, A&A, 421, 83
Romero G. E., Cellone S. A., Combi J. A., 1999, A&AS, 135, 477
Romero G. E., Cellone S. A., Combi J. A., Andruchow I., 2002, A&A, 390, 431
Scarpa R., Urry C. M., Padovani P., Calzetti D., O'Dowd M., 2000, ApJ, 544, 258
Schlegel D. J., Finkbeiner D. P., Davis M., 1998, ApJ, 500, 525
Speziali R., Natali G., 1998, A&A, 339, 382
Stalin C. S., Gopal Krishna, Sagar R., Wiita P. J., 2004, JA&A, 25, 1
Stalin C. S., Gopal-Krishna, Sagar R., Wiita P. J., Mohan V., Pandey A. K., 2006, MNRAS, 366, 1337
Tosti G. et al., 1999, Blazar Data, 2, 1
Vermeulen R. C., Ogle P. M., Tran H. D., Browne I. W. A., Cohen M. H., Readhead A. C. S., Taylor G. B., Goodrich R. W., 1995, ApJ, 452, L5
Villata M., Raiteri C. M., Lanteri L., Sobrito G., Cavallone M., 1998, A&AS, 130, 305
Villata M. et al., 2002, A&A, 390, 407
Villata M. et al., 2004, A&A, 421, 103
Villata M. et al., 2009, A&A, 501, 455
Wagner S. J., Witzel A., 1995, ARA&A, 33, 163
Wierzcholska A., Ostrowski M., Stawarz Ł., Wagner S., Hauser M., 2015, A&A, 573, A69

This paper has been typeset from a T_EX/L^AT_EX file prepared by the author.